BIOCHEMISTRY
including biophysical chemistry & molecular biology

Article

pubs.acs.org/biochemistry

NBD-Labeled Phospholipid Accelerates Apolipoprotein C-II Amyloid Fibril Formation but Is Not Incorporated into Mature Fibrils

Timothy M. Ryan,[†] Michael D. W. Griffin,[†] Michael F. Bailey,[†] Peter Schuck,[‡] and Geoffrey J. Howlett*,[†]

[†]Department of Biochemistry and Molecular Biology, Bio21 Molecular Science and Biotechnology Institute, The University of Melbourne, Melbourne, Victoria 3010, Australia

[‡]Dynamics of Macromolecular Assembly Section, Laboratory of Cellular Imaging and Macromolecular Biophysics, National Institute of Biomedical Imaging and Bioengineering, National Institutes of Health, Bethesda, Maryland 20892, United States

ABSTRACT: Human apolipoprotein (apo) C-II is one of several lipid-binding proteins that self-assemble into fibrils and accumulate in disease-related amyloid deposits. A general characteristic of these amyloid deposits is the presence of lipids, known to modulate individual steps in amyloid fibril formation. ApoC-II fibril formation is activated by submicellar phospholipids but inhibited by micellar lipids. We examined the mechanism for the activation by submicellar lipids using the fluorescently labeled, short-chain phospholipid 1-dodecyl-[(7-nitro-2-1,3-benzoxadiazol-4-yl)amino]-2-hydroxyglycero-3-phosphocholine (NBD-lyso-12-PC). Addition of submicellar NBD-lyso-12-PC increased the rate of fibril formation by apoC-II approximately 2-fold. Stopped flow kinetic analysis using fluorescence detection and low, non-fibril-forming concentrations of apoC-II indicated NBD-lyso-12-PC binds rapidly, on the millisecond time scale, followed by the slower formation of discrete apoC-II tetramers. Sedimentation velocity analysis showed NBD-lyso-12-PC binds to both apoC-II monomers and tetramers at approximately five sites per monomer with an average dissociation constant of approximately 10 μM. Mature apoC-II fibrils formed in the presence of NBD-lyso-12-PC were devoid of lipid, indicating a purely catalytic role for submicellar lipids in the activation of apoC-II fibril formation. These studies demonstrate the catalytic potential of small amphiphilic molecules in controlling protein folding and fibril assembly pathways.

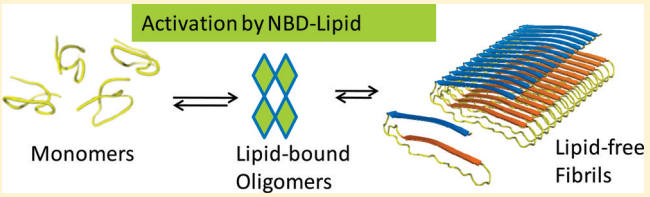

The aggregation of proteins into amyloid fibrils is associated with a wide variety of diseases, ranging from neurodegenerative Alzheimer's and Parkinson's diseases to systemic amyloidoses.[1] The formation of these fibrillar aggregates appears to be a general feature of proteins, as more than 20 individual proteins form amyloid in vivo,[2] while several other proteins readily form amyloid fibrils in vitro under a variety of solution conditions.[1] Amyloid deposits in vivo also contain nonfibrillar material, including the amyloid specific proteins apolipoprotein (apo) E and serum amyloid P, proteoglycans, and lipids.[2,3] The importance of lipids in amyloid deposits is underscored by the number of reports of lipid modulation of amyloid fibril formation. Several studies[4−12] have noted that the effect of lipids depends on the lipid:protein ratio and the nature of the interaction between the polypeptide and the lipid surface. Insertion of the protein into the surface inhibits fibril formation,[4] while transient electrostatic interactions can enhance the process by increasing the local protein concentration and providing a scaffold for amyloid prone conformations.[13] Studies with micellar and submicellar lipids provide an alternate approach to the analysis of the effects of lipids on amyloid fibril formation and permit the role of individual lipid molecules to be examined.[10,12,14]

Apolipoproteins are lipid binding proteins that constitute a high proportion of the proteins that form amyloid in vivo. ApoA-I, apoA-II, and apoC-II are deposited in atherosclerotic lesions and may contribute to the progression of cardiovascular diseases.[15−18] In addition, amyloid formation by apoA-I, apoA-II, and apoA-IV is associated with several hepatic, systemic, and renal amyloid diseases.[19−24] Human apoC-II is an 8914 Da exchangeable apolipoprotein that associates with VLDL and chylomicrons, where it acts as a cofactor for lipoprotein lipase. In the presence of micellar lipid mimetics, apoC-II adopts a predominantly α-helical structure.[25,26] Conversely, lipid-free apoC-II rapidly self-assembles into homogeneous fibrils with increased levels of β-structure and all of the hallmarks of amyloid.[27] A structural model of apoC-II fibrils composed of a linear assembly of monomers in a "letter G-like" conformation has recently been described.[28]

ApoC-II amyloid fibril formation is inhibited by micellar concentrations of phospholipids such as dihexanoylphosphatidylcholine (DHPC), whereas submicellar DHPC enhances fibril formation via the induction of a tetrameric intermediate that acts as a nucleus for fibril elongation.[29−31] Screening a large number of lipids and related amphiphiles at submicellar concentrations identified a range of activators and inhibitors of apoC-II fibril formation.[32] Biophysical studies showed that activators promoted the formation of a tetrameric intermediate enriched in β-structure, while inhibitors induced dimeric

Received: August 1, 2011
Revised: October 3, 2011
Published: October 10, 2011

species with an increased level of α-structure. To further investigate the mechanism for the effects of lipid modulators on amyloid fibril formation pathways, we have used the fluorescently labeled, short-chain phospholipid 1-dodecyl-[(7-nitro-2-1,3-benzoxadiazol-4-yl)amino]-2-hydroxyglycero-3-phosphocholine (NBD-lyso-12-PC). Our results show that apoC-II monomers and tetramers bind several molecules of lipid while mature fibrils are essentially lipid-free. The observation that apoC-II fibrils formed in the presence of NBD-lyso-12-PC lack bound fluorescence indicates that activation by NBD-lyso-12-PC is catalytic with the release of monomer and tetramer bound lipid accompanying fibril elongation and growth.

EXPERIMENTAL PROCEDURES

Alexa 594 C_5 maleimide was obtained from Invitrogen-Molecular Probes (Eugene, OR), and 1-dodecyl-[(7-nitro-2-1,3-benzoxadiazol-4-yl)amino]lauroyl-2-hydroxy-*sn*-glycero-3-phosphocholine (NBD-lyso-12-PC) was obtained from Avanti Polar Lipids, Inc. (Alabaster, AL). ApoC-II was expressed and purified as described previously.[12] Purified apoC-II stock solutions were stored in 5 M guanidine hydrochloride and 10 mM Tris-HCl (pH 8.0) at a concentration of approximately 45 mg/mL. ApoC-II_{S61C} was provided by C. Pham (The University of Melbourne) and was conjugated with Alexa 594 as described previously.[29] ApoC-II lipid interactions and fibril formation were performed by dilution of the stock apoC-II solution into refolding buffer [100 mM sodium phosphate and 0.1% sodium azide (pH 7.4)].

Fluorescence Measurements. The time course of fibril formation was determined using a previously described centrifugal pelleting assay,[29] where the proportion of non-sedimenting material in the supernatant was measured using tryptophan fluorescence (excitation at 295 nm, emission at 350 nm). Fluorescence resonance energy transfer (FRET) between NBD-lyso-12-PC and Alexa 594-labeled apoC-II was measured using a Cary Eclipse instrument (Varian, Palo Alto, CA), with excitation at 430 nm and emission spectra collected from 450 to 750 nm. Stopped flow measurements were conducted using an RX-6200 portable stopped flow device (Applied Photophysics, Leatherhead, Surrey, U.K.) equipped with a pneumatic drive and 2 × 2 mL syringes for the ligand and acceptor solutions. In all cases, stopped flow was conducted using a stopping volume of 150 μL. A pelleting assay, described previously for measuring the interaction of HDL with apoC-II amyloid fibrils,[33] was used to test whether NBD-lyso-12-PC binds to apoC-II fibrils. Briefly, apoC-II fibrils (0.3 mg/mL) in the presence and absence of NBD-lyso-12-PC were layered onto a 20% sucrose cushion and centrifuged for 30 min at 100000 rpm (436000*g*) in an OptimaMax centrifuge using a TLA-100 rotor (Beckman Coulter Instruments, Inc., Fullerton, CA). The original sample, pellet, and supernatant fractions were assayed for NBD fluorescence.

Sedimentation Velocity Analysis. Sedimentation velocity experiments were conducted using an AnTi50 rotor and analytical ultracentrifuge cells equipped with quartz windows and double-sector charcoal Epon centerpieces. Sedimentation velocity experiments for apoC-II alone were conducted using optical density measurements at 280 nm. Fluorescence detection sedimentation experiments were conducted using an XL-A analytical ultracentrifuge (Beckman Coulter Instruments, Inc.) equipped with a fluorescence detection system (FDS; Aviv Associates Inc.). Sedimentation velocity data for NBD-lyso-12-PC in the absence and presence of unlabeled apoC-II or apoC-II fibrils were obtained at 20 °C using a rotor speed of 50000 rpm (180000*g*). Fluorescence data were collected at 1 min intervals from 6.0 to 7.25 cm with the excitation laser focused to a spot 20 μm in diameter, 31 μm below the surface of the sapphire window. Sedimentation velocity data obtained from these experiments were analyzed using the $c(s)$ model in SEDFIT9.4.[34,35] Data for the concentration dependence of the weight-average sedimentation coefficient of apoC-II in the presence of NBD-lyso-12-PC were analyzed according to a reversible monomer−tetramer equilibrium model assuming sedimentation coefficients of 0.93 and 2 S for the apoC-II monomer and tetramer, respectively.[29] For these calculations, data collected at apoC-II concentrations of <1 μM were omitted because of significant overlap of fluorescence from nonsedimenting NBD-lyso-12-PC.

RESULTS

Submicellar NBD-lyso-12-PC Activates ApoC-II Fibril Formation. The critical micelle concentration (CMC) for NBD-lyso-12-PC was determined from the intensity of scattered 600 nm light as a function of NBD-lyso-12-PC concentration (Figure 1A). The data show a shallow linear gradient at low concentrations of NBD-lyso-12-PC followed by a much steeper gradient at higher concentrations. The break

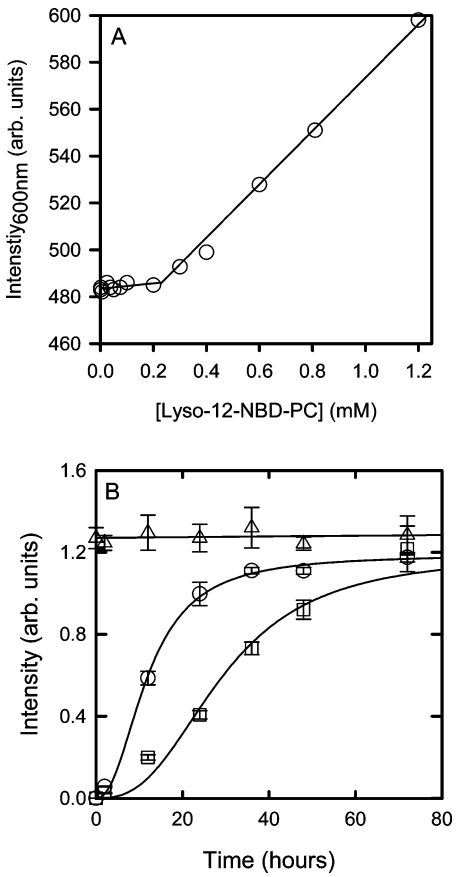

Figure 1. Effect of submicellar NBD-lyso-12-PC on apoC-II fibril formation. (A) Determination of CMC for NBD-lyso-12-PC using light scattering. (B) ApoC-II fibril formation (0.3 mg/mL) monitored using a centrifugal pelleting assay in the absence (□) and presence (○) of NBD-lyso-12-PC (60 μM) and control data where the apoC-II sample with NBD-lyso-12-PC was not centrifuged (△).

dx.doi.org/10.1021/bi201192r | *Biochemistry* 2011, 50, 9579–9586

point between these two lines indicates a CMC of approximately 0.2 mM for NBD-lyso-12-PC. While previous studies have demonstrated the activation of apoC-II fibril formation by submicellar lipids,[29,30] this has not been shown for submicellar NBD-lyso-12-PC. The effect of submicellar NBD-lyso-12-PC on apoC-II amyloid fibril formation was measured using a centrifugal pelleting assay (Figure 1B). ApoC-II (0.3 mg/mL) in the absence of lipid showed a time-dependent increase in the amount of sedimenting material, with a time to half-maximum (t_{50}) of approximately 28 h. Addition of 60 μM NBD-lyso-12-PC reduced the t_{50} to 11.8 h, indicating significant activation, comparable to the effects previously observed with other submicellar phospholipids.[29,30]

NBD-lyso-12-PC Binds Rapidly to ApoC-II Monomers. The association of Alexa 594-labeled apoC-II with NBD-lyso-12-PC was examined using FRET measurements. Figure 2A shows the spectra of NBD-lyso-12-PC alone, Alexa 594-labeled apoC-II alone, and a mixture at the same concentrations of NBD-lyso-12-PC and Alexa 594-labeled apoC-II. The decrease in intensity at 540 nm and the increase in intensity at 620 nm indicate significant transfer of excitation from the NBD fluorophore to the Alexa 594 fluorophore, suggesting an interaction between nonfibrillar apoC-II and NBD-lyso-12-PC. This FRET signal was exploited in examining the millisecond time scale kinetics of the lipid–protein interactions using stopped flow analysis. Figure 2B shows the intensity of NBD-lyso-12-PC at 540 nm upon excitation at 430 nm over time in the presence and absence of Alexa 594-labeled apoC-II. In the absence of Alexa 594-labeled apoC-II, the NBD-lyso-12-PC fluorescence was constant over the time course of the experiment. Addition of Alexa 594-labeled apoC-II induced a rapid decay in the fluorescence intensity, which was complete after 100 ms. The decay in fluorescence intensity due to FRET was dependent on the concentration of labeled apoC-II and indicates a very rapid association of protein with the lipid. These fluorescence decays were globally fitted to provide a pseudo-first-order rate constant of 156000 s^{-1}.

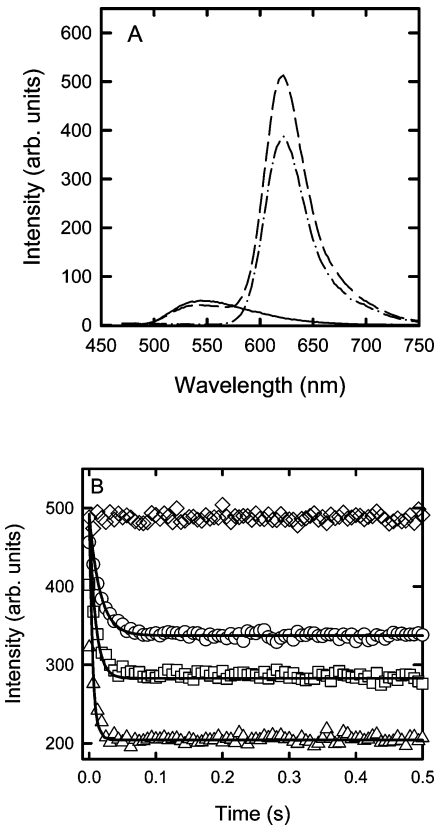

Figure 2. FRET analysis of the interaction between NBD-lyso-12-PC and freshly refolded Alexa 594-labeled apoC-II. (A) Fluorescence spectra using excitation at 430 nm for NBD-lyso-12-PC (60 μM) alone (—), the same concentration of NBD-lyso-12-PC in the presence of Alexa 594-labeled apoC-II (5 μM) (– – –), and Alexa 594-labeled apoC-II (5 μM) alone (–·–). (B) Stopped flow analysis of the interaction of NBD-lyso-12-PC with apoC-II monitored using FRET (excitation at 430 nm, emission at 540 nm). Data obtained using NBD-lyso-12-PC (60 μM) and Alexa 594-labeled apoC-II concentrations of 0 (◇), 1.25 (○), 2.5 (□), and 5 μM (△). The solid lines are global best fits to a pseudo-first-order rate constant.

NBD-lyso-12-PC Binds to Multiple Sites on ApoC-II Monomers and Tetramers. The fluorescence properties of NBD-lyso-12-PC permitted fluorescence detection using the analytical ultracentrifuge to measure the interaction of this lipid with apoC-II, at low non-fibril-forming concentrations of apoC-II. Representative sedimentation velocity data sets (Figure 3A,B) show an increased amount of fluorescence in the sedimenting boundary compared to the nonsedimenting fluorescence as the concentration of apoC-II is increased. Approximate values for the molecular mass and partial specific volume of NBD-lyso-12-PC (0.93 mL/g and 600, respectively) yield a sedimentation coefficient for NBD-lyso-12-PC of <0.06 S, consistent with the observation that this molecule does not sediment appreciably at 50000 rpm (180000*g*). With the small sedimentation coefficient of NBD-lyso-12-PC and the similarity of the sedimentation coefficients of free and NBD-lyso-12-PC-bound apoC-II (see below), the effective particle theory of sedimentation of reacting system [36] shows, supported by simulations, that the nonsedimenting fluorescence in the supernatant provides a reliable estimate of the amount of free NBD-lyso-12-PC in the original solution. Accordingly, the dependence of the nonsedimenting fluorescence on the concentration of added apoC-II (over the range of 0.45–28 μM) was used to obtain the proportion of bound NBD-lyso-12-PC per apoC-II molecule as a function of free lipid (Figure 3C). Analysis of this data, assuming a multiple-site model, yielded a stoichiometry of approximately five lipid molecules per molecule of apoC-II and an intrinsic dissociation constant of approximately 10 μM (Figure 3C). This binding constant may be considered as an average of the affinities of NBD-lyso-12-PC for apoC-II monomers and tetramers, because under the conditions that were used the protein existed as an equilibrium mixture of these two species (see Figure 4).

Sedimentation velocity data using fluorescence detection of NBD-lyso-12-PC over a range of apoC-II concentrations were analyzed using a $c(s)$ model to obtain coefficient distributions (Figure 4A). The distributions at the lower apoC-II concentrations show two distinct peaks at approximately 1 and 2 S, corresponding to the sedimentation coefficients observed for monomeric and tetrameric apoC-II, respectively, formed in the presence of DHPC.[29] Increasing the concentration of apoC-II shifted the distributions toward a single broad peak with a modal sedimentation coefficient of 1.9 S. Because the measured fluorescence signal arises from the lipid component, these distributions indicate that NBD-lyso-12-PC associates with apoC-II and binds to both apoC-II monomers and tetramers.

dx.doi.org/10.1021/bi201192r | *Biochemistry* 2011, 50, 9579–9586

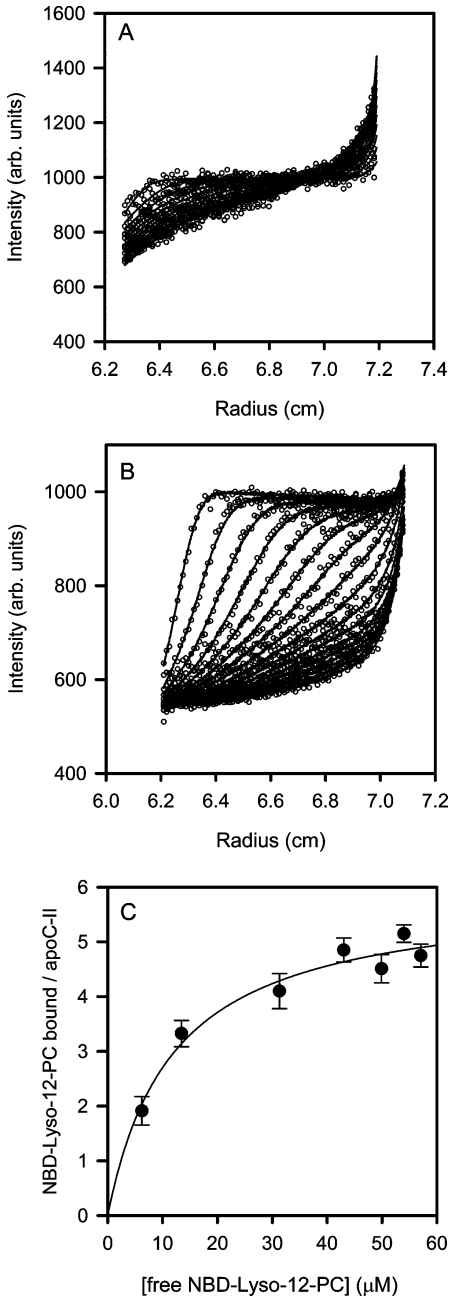

Figure 3. Sedimentation velocity data using fluorescence detection of NBD-lyso-12-PC (60 μM) in the presence of apoC-II at 3.5 and 14 μM (panels A and B, respectively). (C) The molar ratio of bound NBD-lyso-12-PC per apoC-II was estimated from the proportion of nonsedimenting fluorescence material for NBD-lyso-12-PC samples (60 μM) containing a range of apoC-II concentrations (0.45−28 μM). The solid line is the best fit to the data assuming a simple multiple-site binding model.

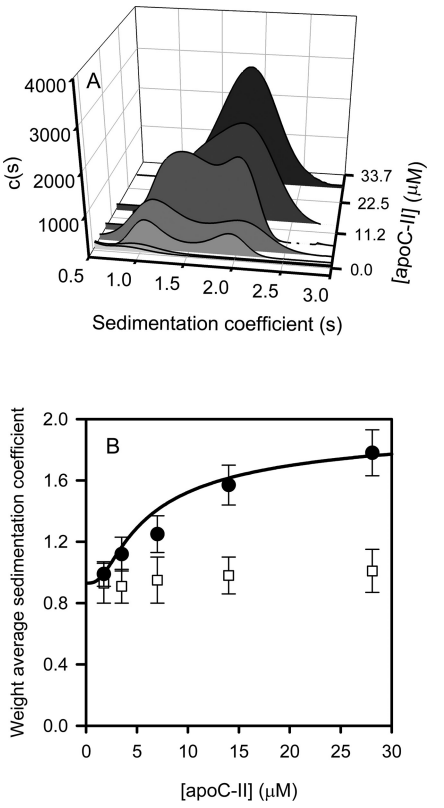

Figure 4. Sedimentation velocity analysis of the interaction between NBD-lyso-12-PC and apoC-II. Sedimentation velocity data using fluorescence detection were obtained for NBD-lyso-12-PC samples (60 μM) containing a range of apoC-II concentrations (0.45−28 μM). (A) Analysis of the data assuming a continuous sedimentation coefficient distribution $c(s)$ model. (B) Weight-average sedimentation coefficients (●), obtained by integration of sedimentation coefficient distributions in panel A. The solid line is a fit to the data assuming a monomer−tetramer model. The weight-average sedimentation coefficients for apoC-II samples alone, monitored by optical density measurements at 280 nm, are shown for comparison (□).

The $c(s)$ distributions in Figure 4 were integrated to obtain signal-weighted average sedimentation coefficients, $s_{w,NBD}$. On the basis of the observation that the fluorescence emission of NBD-lyso-12-PC does not change in the presence of apoC-II (data not shown), this will correspond to the standard weight-average sedimentation coefficient of the ligand-bound species. The sedimentation coefficient for apoC-II alone, detected using optical density measurements, did not display any significant change over the course of the experiment. However, $s_{w,NBD}$ of apoC-II in the presence of NBD-lyso-12-PC displayed an increase that was dependent on apoC-II concentration and consistent with lipid-induced tetramerization. Because of the low sedimentation coefficient of NBD-lyso-12-PC alone, the increasing $s_{w,NBD}$ value cannot be attributed to multiple bound ligands. Analysis of the dependence of the weight-average sedimentation coefficient on apoC-II concentration yielded a value of 3.5×10^{-3} μM^{-3} for the monomer−tetramer equilibrium constant (Figure 4B). This value is similar in magnitude to estimates provided from previous kinetic analyses of DHPC-induced apoC-II tetramerization.[29]

ApoC-II Fibrils Do Not Bind NBD-lyso-12-PC. Our studies of apoC-II fibril formation show that submicellar phospholipids activate fibril nucleation rather than elongation.[37] However, these observations do not preclude interactions between lipid and fibrillar material, which could also play a role in promoting fibril aggregation. It was therefore of interest to determine if phospholipid remained associated with the fibrillar end product. The binding of lipids to apoC-II amyloid fibrils was initially investigated with a FRET assay (Figure 5). The time course for the change in the FRET signal observed for NBD-lyso-12-PC and the monomer and tetramers of Alexa 594-labeled apoC-II (Figure 2) decreased exponentially during incubation under fibril forming conditions, indicative of a loss of bound lipid. The lack of binding of NBD-lyso-12-PC to

dx.doi.org/10.1021/bi201192r | Biochemistry 2011, 50, 9579−9586

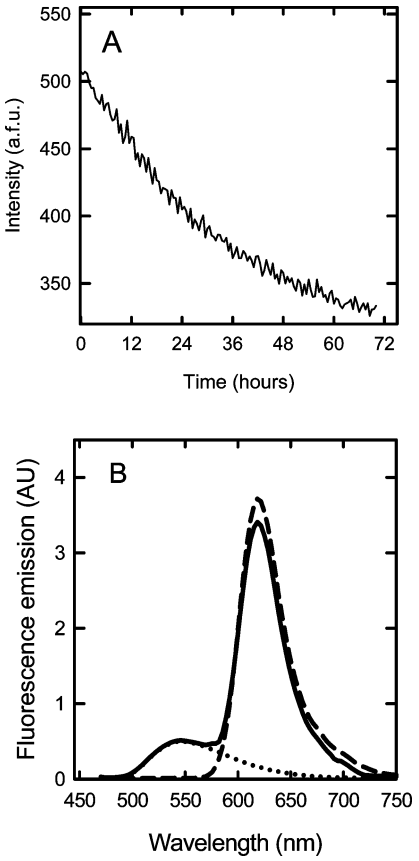

Figure 5. FRET analysis of the interaction between Alexa 594-labeled apoC-II fibrils and NBD-lyso-12-PC. (A) Time course for the change in FRET during apoC-II fibril formation. Alexa 594-labeled apoC-II (33 μM) was incubated with NBD-lyso-12-PC (60 μM) at 20 °C, and the fluorescence emission at 620 nm was measured with excitation at 430 nm. (B) Fluorescence emission spectra (in arbitrary units) for Alexa 594-labeled apoC-II fibrils alone (5 μM) (---), Alexa 594-labeled apoC-II fibrils (5 μM) in the presence of 60 μM NBD-lyso-12-PC (—), and 60 μM NBD-lyso-12-PC alone (···) were acquired using excitation at 430 nm.

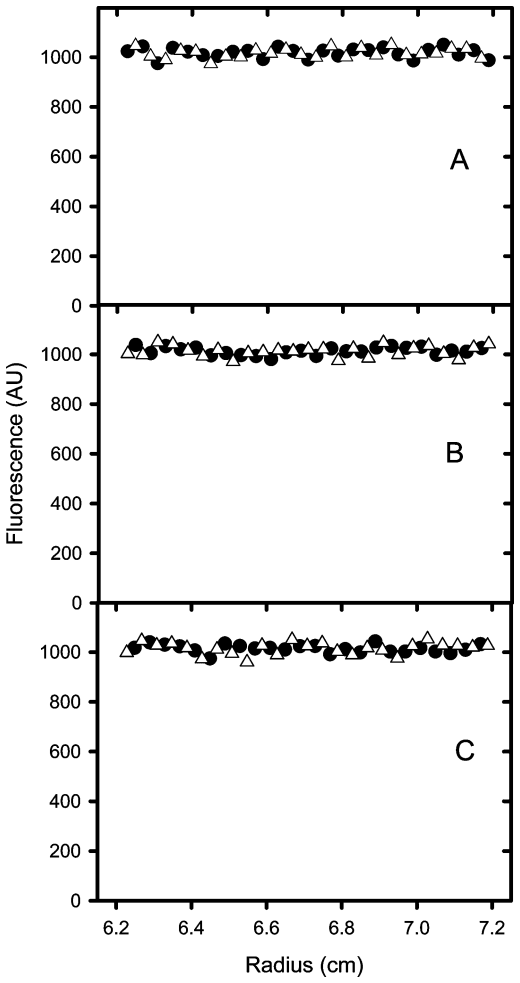

Figure 6. Sedimentation velocity analysis using fluorescence detection of NBD-lyso-12-PC in the presence and absence of apoC-II fibrils. Samples of NBD-lyso-12-PC alone (A) and NBD-lyso-12-PC in the presence of apoC-II fibrils (33 μM) that were either preformed (B) or formed in the presence of NBD-lyso-12-PC (60 μM) by incubation at 20 °C for 5 days (C) were analyzed using fluorescence detection in the analytical ultracentrifuge. The radial scans are for data collected after 20 min (●) and 5 h (△) using a rotor speed of 50000 rpm. For the sake of clarity, only every 40th data point is presented.

apoC-II fibrils was supported by fluorescence emission spectra that showed no significant increase in intensity at 620 nm, indicating that there is little or no FRET between NBD-lyso-12-PC and Alexa 594-labeled fibrillar apoC-II (Figure 5). This result was confirmed by sedimentation velocity analysis using the FDS; no significant sedimentation was observed at 50000 rpm (4600*g*) for either NBD-lyso-12-PC alone (60 μM) or NBD-lyso-12-PC in the presence of apoC-II fibrils (33 μM), which were either preformed or formed in the presence of NBD-lyso-12-PC (Figure 6). Further confirmation of the lack of an interaction between NBD-lyso-12-PC and apoC-II amyloid fibrils was provided by a centrifugal pelleting assay using a 20% sucrose cushion to separate free lipid from bound lipid (Table 1). This assay has previously been used to identify the binding of HDL particles to apoC-II fibrils.[33] NBD-lyso-12-PC alone (60 μM) did not pellet through the sucrose solution, as the control without any fibrillar material contained <0.0003% of the fluorescence contained in the original solution and supernatant fractions. A similar low level of fluorescence in the pellet fraction was observed for NBD-lyso-12-PC solutions containing preformed apoC-II amyloid fibrils or apoC-II fibrils formed in the presence of NBD-lyso-12-PC. Control experiments using apoC-II in the absence of NBD-lyso-12-PC displayed no fluorescence either before or after centrifugation.

DISCUSSION

Amphipathic lipids and lipid mimetics affect several amyloid-forming systems[4−12] with no obvious pattern concerning the magnitude and specificities of the effects observed. In the case of apoC-II, submicellar concentrations of short-chain phospholipids[29,31] and oxidized cholesterol[38] activate apoC-II fibril formation whereas low concentrations of micellar lipids and lipid bilayers, while initially inhibiting fibril formation, ultimately induce apoC-II fibrils with a distinctive straight rodlike morphology.[30] The complexity of the interactions of apoC-II with lipids is further illustrated by the results of a screen of amphipathic molecules that indentified a range of submicellar modulators that exerted independent effects on fibril nucleation and elongation.[32] These results provide new insight into the apoC-II−lipid interaction, revealing multiple lipid binding sites. The results are consistent with mass

dx.doi.org/10.1021/bi201192r | *Biochemistry* 2011, 50, 9579−9586

Table 1. Sedimentation Analysis of NBD-lyso-12-PC in the Presence and Absence of ApoC-II Fibrils[a]

sample	original sample	supernatant	pellet fraction
NBD-lyso-12-PC alone	1	1	2.16×10^{-6}
NBD-lyso-12-PC with preformed apoC-II fibrils	1	1	2.26×10^{-6}
apoC-II fibrils formed in the presence of NBD-lyso-12-PC	1	1	2.23×10^{-6}
apoC-II fibrils alone	2.20×10^{-6}	2.20×10^{-6}	2.19×10^{-6}

[a]Samples of NBD-lyso-12-PC (60 μM) were prepared in the absence and presence of apoC-II fibrils (33 μM) that were either preformed or formed in the presence of NBD-lyso-12-PC by incubation at 20 °C for 5 days. The samples were centrifuged at 100000 rpm (436000*g*) in a preparative ultracentrifuge for 30 min, and the fluorescence emission of NBD-lyso-12-PC (60 μM) was determined for the original solution, the supernatant, and pellet fractions made up to the original volume. Fluorescence emission is expressed relative to that of the initial NBD-lyso-12-PC solution.

spectrometry studies of apoC-II with lipids in the gas phase that also indicate multiple lipid-bound apoC-II species.[39] The existence of multiple lipid binding sites suggests the diversity of the effects of lipids on apoC-II fibril formation may depend on the occupancy of specific sites and the role the individual sites play in the fibril assembly process.

Our previous studies have shown that the activation of apoC-II fibril formation by DHPC occurs by the rapid induction of a discrete tetramer followed by a slow isomerization of the tetramer that precedes accelerated fibril growth.[29] Activation by NBD-lyso-12-PC appears to follow this pattern with the rapid binding of NBD-lyso-12-PC accompanied by the formation of discrete tetramers. An important observation is that although NBD-lyso-12-PC is bound to apoC-II oligomers the final mature fibrils are devoid of bound lipid. Figure 7 summarizes

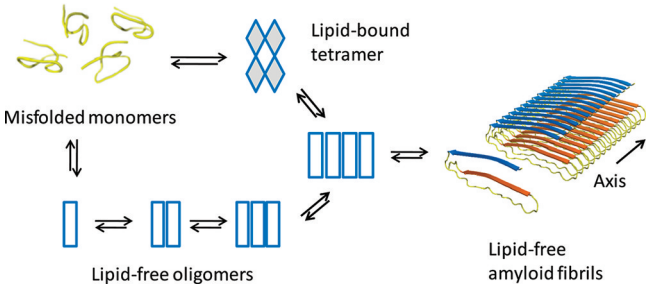

Figure 7. Model for lipid induction of apoC-II fibril assembly. The model proposes a lipid-induced tetramerization followed by a slow isomerization and loss of lipid to generate a nucleus for subsequent fibril elongation. An alternate slower pathway available to lipid-free apoC-II proposes an initial isomerization of apoC-II to form a monomeric nucleus that self-assembles into fibrils. The model for apoC-II fibrils shows a linear assembly of monomers in a letter G-like conformation as recently described.[28]

possible pathways for explaining these observations. One pathway, available to lipid-free apoC-II, involves the slow isomerization of misfolded monomers to generate species competent to rapidly assemble into mature fibrils. Evidence of this pathway is provided by studies of cross-linked apoC-II dimers, which accelerate apoC-II fibril formation.[40] An alternate, NBD-lyso-12-PC-induced pathway is postulated to involve the formation of a tetrameric intermediate that nucleates fibril formation via the slow formation of a lipid-free apoC-II tetramer. The slow isomerization of the apoC-II tetramer is based on previous studies of a slow step in the DHPC-induced acceleration of apoC-II fibril formation.[29] While the molecular details of the initial NBD-lyso-12-PC tetramer complex remain unclear, a possible mechanism for the formation of this species would be a sequential process involving the transient formation of lipid-stabilized dimers followed by self-assembly to form tetrahedral "dimer-of-dimers" structures. According to this model, we propose that the slow isomerization of this tetrahedral structure is accompanied by lipid loss to generate a linear tetramer that serves as a nucleus for fibril elongation.

A number of naturally occurring compounds are known to affect protein folding, including osmolytes such as trehalose that act in the molar concentration range (0.5−1 M), primarily by nonspecific, nonideality effects.[41] A recent example is the effects of the osmolytes TMAO, proline, and glycine-betaine on the Huntington fibril forming pathway.[42] Our previous work identified high-affinity amphipathic activators and inhibitors of human apolipoprotein (apo) C-II fibril formation, active in the micromolar concentration range, including a number of physiological metabolites.[32,38] Other disease-related proteins for which amyloid fibril formation is affected by tight binding amphiphiles include α-synuclein,[43] apoA-I,[44] Aβ,[4] β2-microglobulin,[9] islet amyloid polypeptide,[13] prions,[45] transthyretin,[46] and medin.[47] The importance of this study is the demonstration that submicellar NBD-lyso-12-PC activates apoC-II amyloid fibril formation without being incorporated into the final product. This suggests that low-molecular weight metabolites could play hitherto unrecognized catalytic roles in protein folding and assembly with the potential to modulate aberrant protein misfolding and disease.

AUTHOR INFORMATION

Corresponding Author

*Department of Biochemistry and Molecular Biology, The University of Melbourne, Melbourne, Victoria 3010, Australia. Phone: +61 3 83442271. Fax: +61 3 9348 1421. E-mail: ghowlett@unimelb.edu.au.

Funding

This research was supported under the Australian Research Council's Discovery Projects funding scheme (Project DP0984565). M.D.W.G. is the recipient of an Australian Research Council Post Doctoral Fellowship (Project DP110103528). This work was supported in part by the Intramural Research Program of the National Institute of Biomedical Imaging and Bioengineering, National Institutes of Health.

ABBREVIATIONS

apo, apolipoprotein; CMC, critical micelle concentration; FDS, fluorescence detection system; FRET, fluorescence resonance energy transfer; NBD-lyso-12-PC, 1-dodecyl-[(7-nitro-2-1,3-benzoxadiazol-4-yl)amino]lauroyl-2-hydroxy-*sn*-glycero-3-phosphocholine; ThT, thioflavin T.

REFERENCES

(1) Chiti, F., and Dobson, C. M. (2006) Protein misfolding, functional amyloid, and human disease. *Annu. Rev. Biochem.* 75, 333−366.

(2) Sipe, J. D., and Cohen, A. S. (2000) Review: History of the amyloid fibril. *J. Struct. Biol. 130*, 88−98.
(3) Gellermann, G. P., Appel, T. R., Tannert, A., Radestock, A., Hortschansky, P., Schroeckh, V., Leisner, C., Lutkepohl, T., Shtrasburg, S., Rocken, C., Pras, M., Linke, R. P., Diekmann, S., and Fandrich, M. (2005) Raft lipids as common components of human extracellular amyloid fibrils. *Proc. Natl. Acad. Sci. U.S.A. 102*, 6297−6302.
(4) Bokvist, M., Lindstrom, F., Watts, A., and Grobner, G. (2004) Two types of Alzheimer's β-amyloid (1−40) peptide membrane interactions: Aggregation preventing transmembrane anchoring versus accelerated surface fibril formation. *J. Mol. Biol. 335*, 1039−1049.
(5) Chirita, C. N., Necula, M., and Kuret, J. (2003) Anionic micelles and vesicles induce tau fibrillization in vitro. *J. Biol. Chem. 278*, 25644−25650.
(6) Gorbenko, G. P., and Kinnunen, P. K. (2006) The role of lipid-protein interactions in amyloid-type protein fibril formation. *Chem. Phys. Lipids 141*, 72−82.
(7) Necula, M., Chirita, C. N., and Kuret, J. (2003) Rapid anionic micelle-mediated α-synuclein fibrillization in vitro. *J. Biol. Chem. 278*, 46674−46680.
(8) Ookoshi, T., Hasegawa, K., Ohhashi, Y., Kimura, H., Takahashi, N., Yoshida, H., Miyazaki, R., Goto, Y., and Naiki, H. (2008) Lysophospholipids induce the nucleation and extension of β2-microglobulin-related amyloid fibrils at a neutral pH. *Nephrol., Dial., Transplant. 23*, 3247−3255.
(9) Pal-Gabor, H., Gombos, L., Micsonai, A., Kovacs, E., Petrik, E., Kovacs, J., Graf, L., Fidy, J., Naiki, H., Goto, Y., Liliom, K., and Kardos, J. (2009) Mechanism of lysophosphatidic acid-induced amyloid fibril formation of β_2-microglobulin in vitro under physiological conditions. *Biochemistry 48*, 5689−5699.
(10) Rangachari, V., Reed, D. K., Moore, B. D., and Rosenberry, T. L. (2006) Secondary structure and interfacial aggregation of amyloid-β(1−40) on sodium dodecyl sulfate micelles. *Biochemistry 45*, 8639−8648.
(11) Shao, H., Jao, S., Ma, K., and Zagorski, M. G. (1999) Solution structures of micelle-bound amyloid β(1−40) and β(1−42) peptides of Alzheimer's disease. *J. Mol. Biol. 285*, 755−773.
(12) Yamamoto, S., Hasegawa, K., Yamaguchi, I., Tsutsumi, S., Kardos, J., Goto, Y., Gejyo, F., and Naiki, H. (2004) Low concentrations of sodium dodecyl sulfate induce the extension of β2-microglobulin-related amyloid fibrils at a neutral pH. *Biochemistry 43*, 11075−11082.
(13) Knight, J. D., and Miranker, A. D. (2004) Phospholipid catalysis of diabetic amyloid assembly. *J. Mol. Biol. 341*, 1175−1187.
(14) Sureshbabu, N., Kirubagaran, R., and Jayakumar, R. (2009) Surfactant-induced conformational transition of amyloid β-peptide. *Eur. Biophys. J. 38*, 355−367.
(15) Westermark, P., Mucchiano, G., Marthin, T., Johnson, K. H., and Sletten, K. (1995) Apolipoprotein A1-derived amyloid in human aortic atherosclerotic plaques. *Am. J. Pathol. 147*, 1186−1192.
(16) Mucchiano, G. I., Haggqvist, B., Sletten, K., and Westermark, P. (2001) Apolipoprotein A-1-derived amyloid in atherosclerotic plaques of the human aorta. *J. Pathol. 193*, 270−275.
(17) Mucchiano, G. I., Jonasson, L., Haggqvist, B., Einarsson, E., and Westermark, P. (2001) Apolipoprotein A-I-derived amyloid in atherosclerosis. Its association with plasma levels of apolipoprotein A-I and cholesterol. *Am. J. Clin. Pathol. 115*, 298−303.
(18) Medeiros, L. A., Khan, T., El Khoury, J. B., Pham, C. L., Hatters, D. M., Howlett, G. J., Lopez, R., O'Brien, K. D., and Moore, K. J. (2004) Fibrillar amyloid protein present in atheroma activates CD36 signal transduction. *J. Biol. Chem. 279*, 10643−10648.
(19) Bergstrom, J., Murphy, C., Eulitz, M., Weiss, D. T., Westermark, G. T., Solomon, A., and Westermark, P. (2001) Codeposition of apolipoprotein A-IV and transthyretin in senile systemic (ATTR) amyloidosis. *Biochem. Biophys. Res. Commun. 285*, 903−908.
(20) Coriu, D., Dispenzieri, A., Stevens, F. J., Murphy, C. L., Wang, S., Weiss, D. T., and Solomon, A. (2003) Hepatic amyloidosis resulting from deposition of the apolipoprotein A-I variant Leu75Pro. *Amyloid 10*, 215−223.
(21) Yazaki, M., Liepnieks, J. J., Barats, M. S., Cohen, A. H., and Benson, M. D. (2003) Hereditary systemic amyloidosis associated with a new apolipoprotein AII stop codon mutation Stop78Arg. *Kidney Int. 64*, 11−16.
(22) Obici, L., Bellotti, V., Mangione, P., Stoppini, M., Arbustini, E., Verga, L., Zorzoli, I., Anesi, E., Zanotti, G., Campana, C., Vigano, M., and Merlini, G. (1999) The new apolipoprotein A-I variant Leu(174) → Ser causes hereditary cardiac amyloidosis, and the amyloid fibrils are constituted by the 93-residue N-terminal polypeptide. *Am. J. Pathol. 155*, 695−702.
(23) Obici, L., Franceschini, G., Calabresi, L., Giorgetti, S., Stoppini, M., Merlini, G., and Bellotti, V. (2006) Structure, function and amyloidogenic propensity of apolipoprotein A-I. *Amyloid 13*, 191−205.
(24) Bergstrom, J., Murphy, C. L., Weiss, D. T., Solomon, A., Sletten, K., Hellman, U., and Westermark, P. (2004) Two different types of amyloid deposits—apolipoprotein A-IV and transthyretin—in a patient with systemic amyloidosis. *Lab. Invest. 84*, 981−988.
(25) MacRaild, C. A., Hatters, D. M., Howlett, G. J., and Gooley, P. R. (2001) NMR structure of human apolipoprotein C-II in the presence of sodium dodecyl sulfate. *Biochemistry 40*, 5414−5421.
(26) MacRaild, C. A., Howlett, G. J., and Gooley, P. R. (2004) The structure and interactions of human apolipoprotein C-II in dodecyl phosphocholine. *Biochemistry 43*, 8084−8093.
(27) Hatters, D. M., MacPhee, C. E., Lawrence, L. J., Sawyer, W. H., and Howlett, G. J. (2000) Human apolipoprotein C-II forms twisted amyloid ribbons and closed loops. *Biochemistry 39*, 8276−8283.
(28) Teoh, C. L., Pham, C. L., Todorova, N., Hung, A., Lincoln, C. N., Lees, E., Lam, Y. H., Binger, K. J., Thomson, N. H., Radford, S. E., Smith, T. A., Muller, S. A., Engel, A., Griffin, M. D., Yarovsky, I., Gooley, P. R., and Howlett, G. J. (2011) A structural model for apolipoprotein C-II amyloid fibrils: Experimental characterization and molecular dynamics simulations. *J. Mol. Biol. 405*, 1246−1266.
(29) Ryan, T. M., Howlett, G. J., and Bailey, M. F. (2008) Fluorescence detection of a lipid-induced tetrameric intermediate in amyloid fibril formation by apolipoprotein C-II. *J. Biol. Chem. 283*, 35118−35128.
(30) Griffin, M. D., Mok, M. L., Wilson, L. M., Pham, C. L., Waddington, L. J., Perugini, M. A., and Howlett, G. J. (2008) Phospholipid interaction induces molecular-level polymorphism in apolipoprotein C-II amyloid fibrils via alternative assembly pathways. *J. Mol. Biol. 375*, 240−256.
(31) Hatters, D. M., Lawrence, L. J., and Howlett, G. J. (2001) Sub-micellar phospholipid accelerates amyloid formation by apolipoprotein C-II. *FEBS Lett. 494*, 220−224.
(32) Ryan, T. M., Griffin, M. D., Teoh, C. L., Ooi, J., and Howlett, G. J. (2011) High-affinity amphipathic modulators of amyloid fibril nucleation and elongation. *J. Mol. Biol. 406*, 416−429.
(33) Wilson, L. M., Pham, C. L., Jenkins, A. J., Wade, J. D., Hill, A. F., Perugini, M. A., and Howlett, G. J. (2006) High density lipoproteins bind Aβ and apolipoprotein C-II amyloid fibrils. *J. Lipid Res. 47*, 755−760.
(34) Schuck, P. (2000) Size-distribution analysis of macromolecules by sedimentation velocity ultracentrifugation and Lamm equation modeling. *Biophys. J. 78*, 1606−1619.
(35) Schuck, P. (2003) On the analysis of protein self-association by sedimentation velocity analytical ultracentrifugation. *Anal. Biochem. 320*, 104−124.
(36) Schuck, P. (2010) Sedimentation patterns of rapidly reversible protein interactions. *Biophys. J. 98*, 2005−2013.
(37) Ryan, T. M., Griffin, M. D., Teoh, C. L., Ooi, J., and Howlett, G. J. (2011) High-affinity amphipathic modulators of amyloid fibril nucleation and elongation. *J. Mol. Biol. 406*, 416−429.
(38) Stewart, C. R., Wilson, L. M., Zhang, Q., Pham, C. L., Waddington, L. J., Staples, M. K., Stapleton, D., Kelly, J. W., and Howlett, G. J. (2007) Oxidized cholesterol metabolites found in human atherosclerotic lesions promote apolipoprotein C-II amyloid fibril formation. *Biochemistry 46*, 5552−5561.

(39) Hanson, C. L., Ilag, L. L., Malo, J., Hatters, D. M., Howlett, G. J., and Robinson, C. V. (2003) Phospholipid complexation and association with apolipoprotein C-II: Insights from mass spectrometry. *Biophys. J. 85*, 3802−3812.
(40) Pham, C. L., Hatters, D. M., Lawrence, L. J., and Howlett, G. J. (2002) Cross-linking and amyloid formation by N- and C-terminal cysteine derivatives of human apolipoprotein C-II. *Biochemistry 41*, 14313−14322.
(41) Singer, M. A., and Lindquist, S. (1998) Multiple effects of trehalose on protein folding in vitro and in vivo. *Mol. Cell 1*, 639−648.
(42) Borwankar, T., Rothlein, C., Zhang, G., Techen, A., Dosche, C., and Ignatova, Z. (2011) Natural osmolytes remodel the aggregation pathway of mutant huntingtin exon 1. *Biochemistry 50*, 2048−2060.
(43) Stockl, M., Fischer, P., Wanker, E., and Herrmann, A. (2008) α-Synuclein selectively binds to anionic phospholipids embedded in liquid-disordered domains. *J. Mol. Biol. 375*, 1394−1404.
(44) Andreola, A., Bellotti, V., Giorgetti, S., Mangione, P., Obici, L., Stoppini, M., Torres, J., Monzani, E., Merlini, G., and Sunde, M. (2003) Conformational switching and fibrillogenesis in the amyloidogenic fragment of apolipoprotein A-I. *J. Biol. Chem. 278*, 2444−2451.
(45) Deleault, N. R., Harris, B. T., Rees, J. R., and Supattapone, S. (2007) Formation of native prions from minimal components in vitro. *Proc. Natl. Acad. Sci. U.S.A. 104*, 9741−9746.
(46) Zhao, H., Tuominen, E. K., and Kinnunen, P. K. (2004) Formation of amyloid fibers triggered by phosphatidylserine-containing membranes. *Biochemistry 43*, 10302−10307.
(47) Olofsson, A., Borowik, T., Grobner, G., and Sauer-Eriksson, A. E. (2007) Negatively charged phospholipid membranes induce amyloid formation of medin via an α-helical intermediate. *J. Mol. Biol. 374*, 186−194.